Electronic Supplementary Material (ESI) for Catalysis Science & Technology.

Supplementary Information

Catalytic Direct Oxidation of Methane to Methanol by Redox of Copper Mordenite

Junya Ohyama,*[a] Airi Hirayama,[b] Nahoko Kondou,[a] Hiroshi Yoshida,[a] Masato Machida[a] Shun Nishimura,[c] Kazuo Kato,[d] Itsuki Miyazato[e] and Keisuke Takahashi[e]

[a] Faculty of Advanced Science and Technology, Kumamoto University, 2-39-1 Kurokami, Chuo-ku, Kumamoto, 860-8555, Japan

[b] Department of Applied Chemistry and Biochemistry, Graduate School of Science and Technology, Kumamoto University, 2-39-1 Kurokami, Chuo-ku, Kumamoto, 860-8555, Japan

[c] Graduate School of Advanced Science and Technology, Japan Advanced Institute of Science and Technology (JAIST), 1-1 Asahidai, Nomi, 923-1292, Japan

[d] Japan Synchrotron Radiation Research Institute, 1-1 Kouto, Sayo-cho, Sayo-gun Hyogo, 679-5198, Japan

[e] Department of Chemistry, Hokkaido University, N-15 W-8, Sapporo, 060-0815, Japan

* ohyama@kumamoto-u.ac.jp

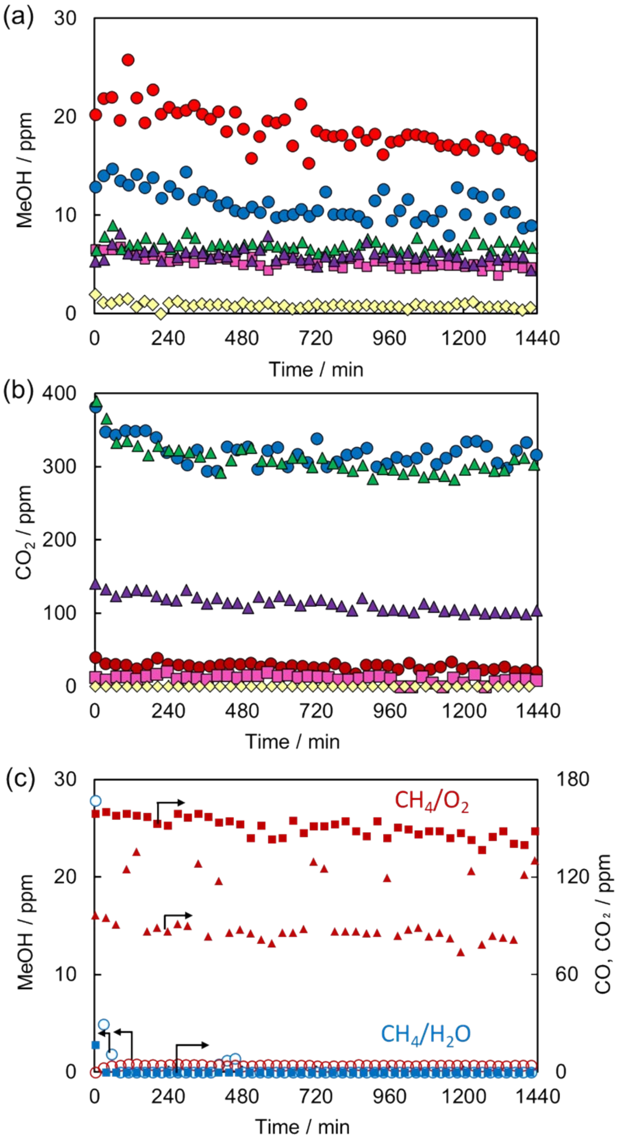

Figure S1 Time courses of (a) CH_3OH and (b) CO_2 production in the $CH_4/O_2/H_2O$ reaction over various Cu zeolites including Cu2.0-MOR10 (red circles), Cu2.3-MOR15 (blue circles), Cu1.4-BEA20 (pink squares), Cu1.1-FAU8 (yellow diamonds), Cu3.3-MFI12 (green triangles), Cu1.5-MFI19 (purple triangles), and H-MOR10 (black circles). $CH_4/O_2/H_2O$ reaction conditions: catalyst 50 mg, 300 °C, CH_4 (48 mL min^{-1}) + O_2 (2 mL min^{-1}) + N_2 (50 mL min^{-1}) + water vapour (H_2O(g); 0.5 g h^{-1}). (c) Time courses of CH_3OH (circles), CO (triangles) and CO_2 (squares) production in the CH_4/O_2 reaction (red) and CH_4/H_2O(g) reaction (blue) over Cu2.0-MOR10. CH_4/O_2 reaction conditions: catalyst 50 mg, 300 °C, CH_4 (48 mL min^{-1}) + O_2 (2 mL min^{-1}) + N_2 (60 mL min^{-1}). CH_4/H_2O(g) reaction conditions: catalyst 50 mg, 300 °C, CH_4 (48 mL min^{-1}) + N_2 (52 mL min^{-1}) + H_2O(g) (0.5 g h^{-1}).

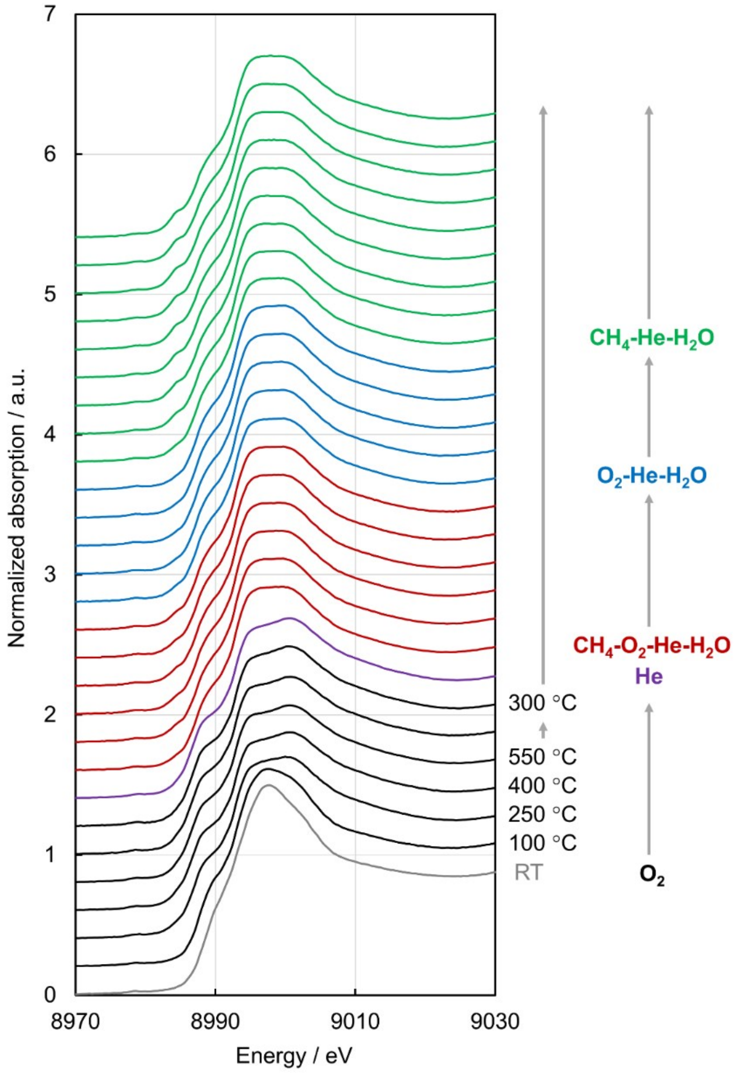

Figure S2 In-situ Cu K-edge XANES spectra of Cu2.0-MOR10 obtained according to Scheme S1. XANES spectra measured before (grey) and after O_2 pretreatment (black) and after exposure to gas flow conditions (1) (red), (2) (blue) and (3) (green).

Scheme S1 Experimental procedure for control in-situ XAFS spectral measurements.

O_2 50 mL min^{-1} at 550 ºC (pretreatment)
↓
Cool to 300 ºC
↓
He 50 mL min^{-1}
↓
CH_4 50 mL min^{-1}
↓
He 100 mL min^{-1}, H_2O(g)
↓
O_2 2 mL min^{-1}, CH_4 48 mL min^{-1}, He 50 mL min^{-1}, H_2O(g)

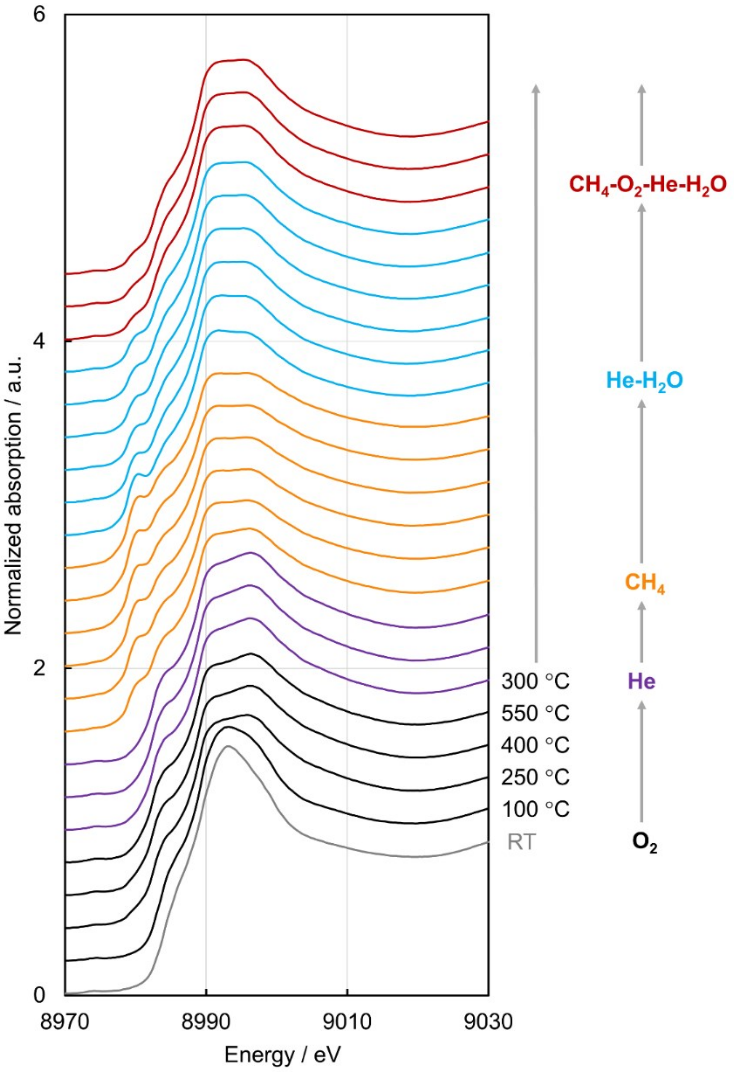

Figure S3 In-situ Cu K-edge XANES spectra of Cu2.0-MOR10 obtained according to Scheme S2.

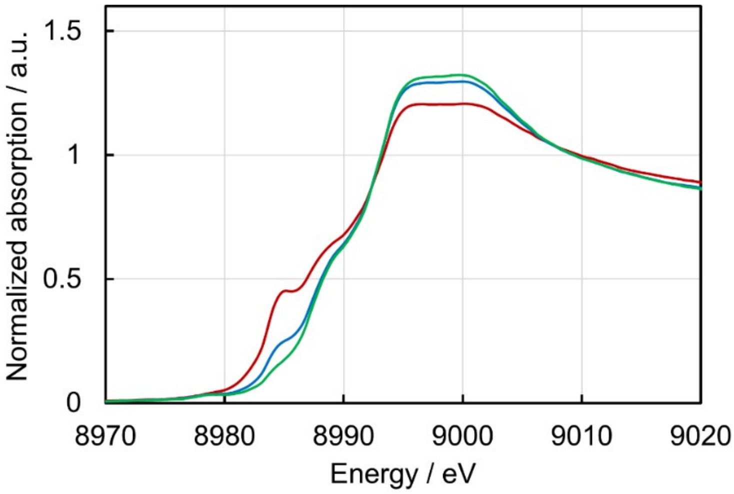

Figure S4 Comparison of the XANES spectra after dry CH_4 (red), wet He (blue) and $CH_4/O_2/H_2O$ gas treatment (green) according to Scheme S2.

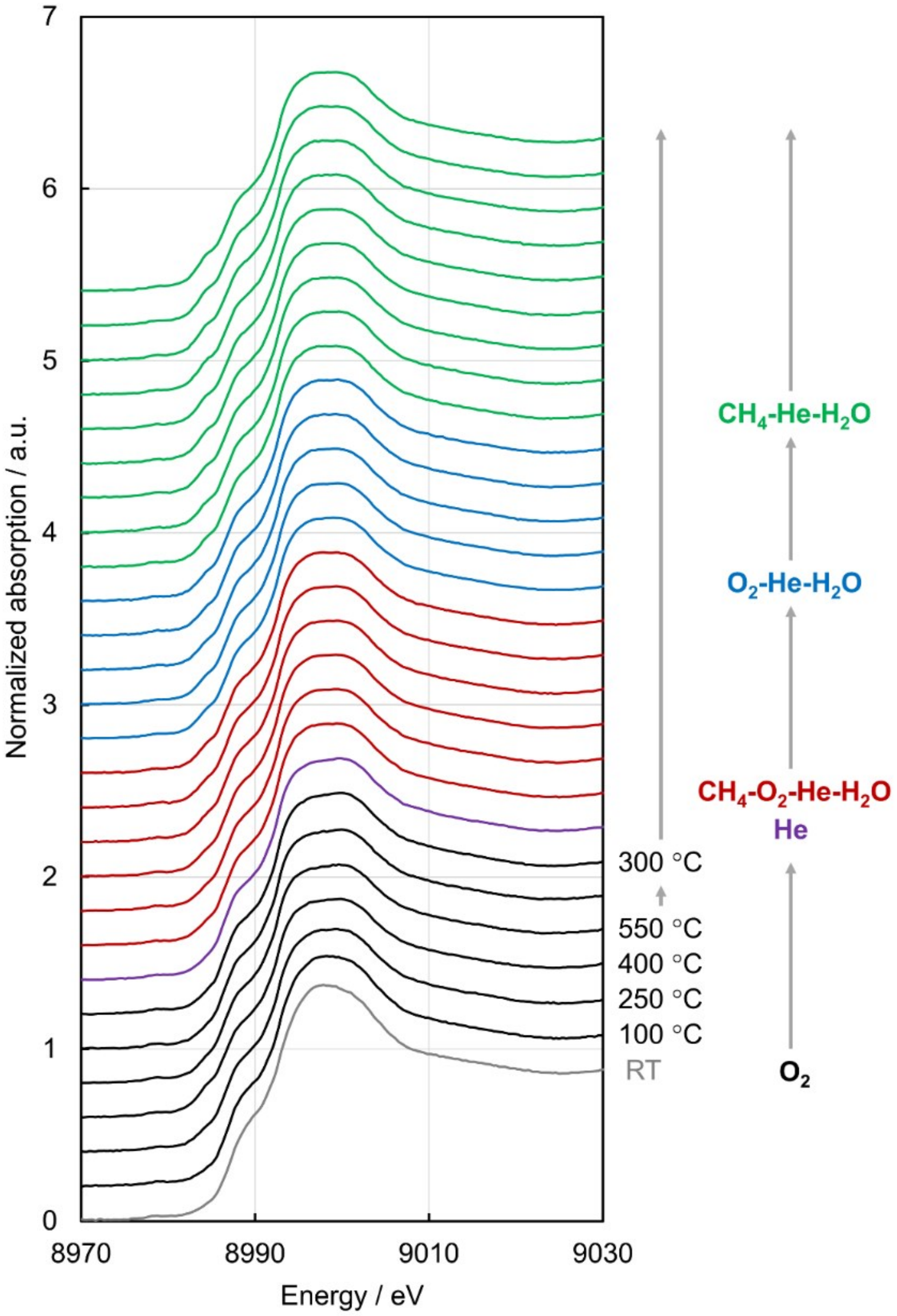

Figure S5 In-situ Cu K-edge XANES spectra of Cu1.1-FAU8 obtained according to Scheme S1. XANES spectra before (grey) and after O_2 pretreatment (black) and those obtained under the gas flow conditions (1) Cu1.1-FAU8 (red), (2) (blue) and (3) (green).

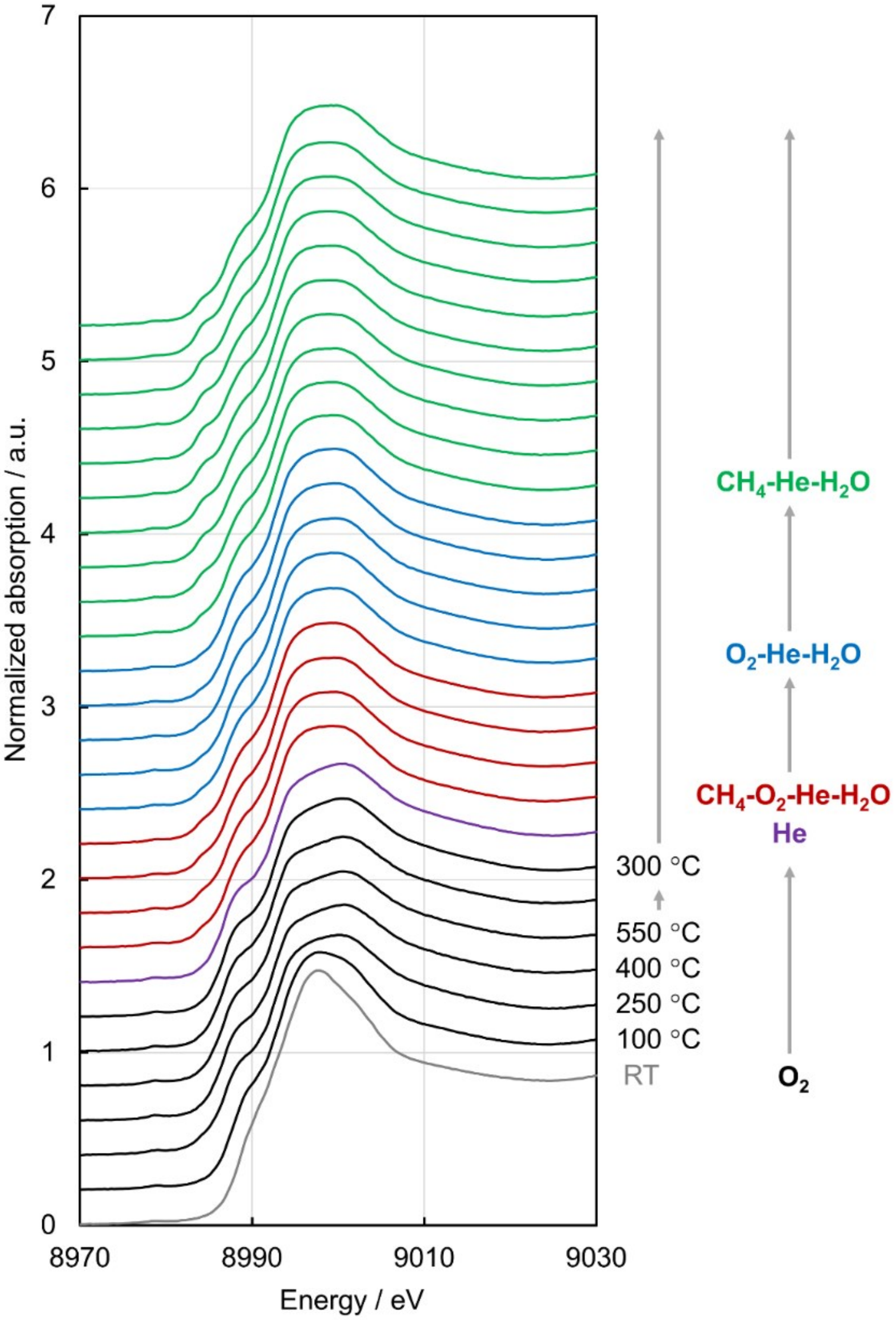

Figure S6 In-situ Cu K-edge XANES spectra of Cu2.3-MOR15 obtained according to Scheme S1. XANES spectra measured before (grey) and after O_2 pretreatment (black) and during exposure to gas flow conditions (1) (red), (2) (blue) and (3) (green).

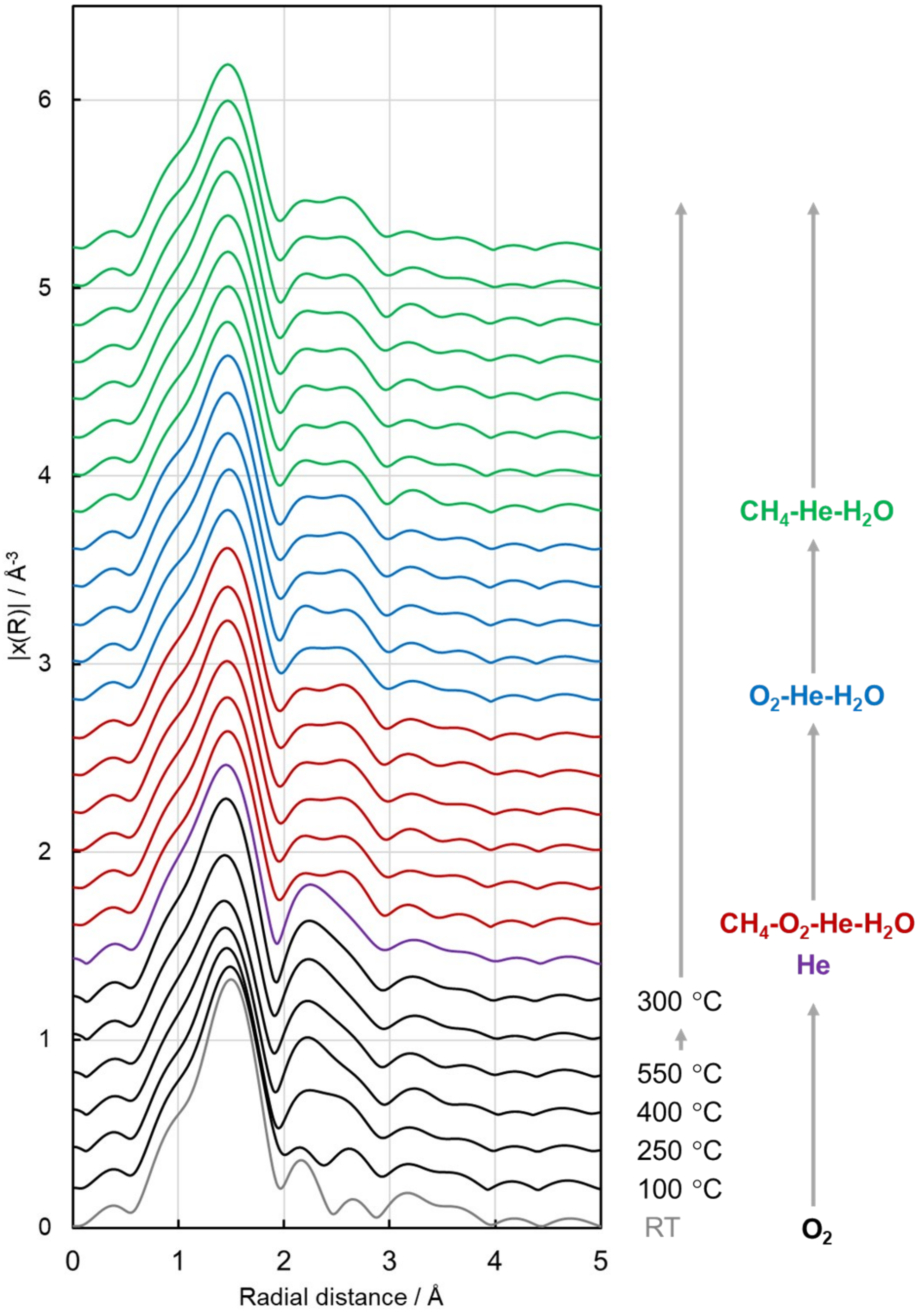

Figure S7 In-situ Cu K-edge FT EXAFS spectra of Cu2.0-MOR10 obtained according to Scheme S1. The EXAFS oscillations are shown in Figure S16(a). FT range: *k* = 3-10 Å.

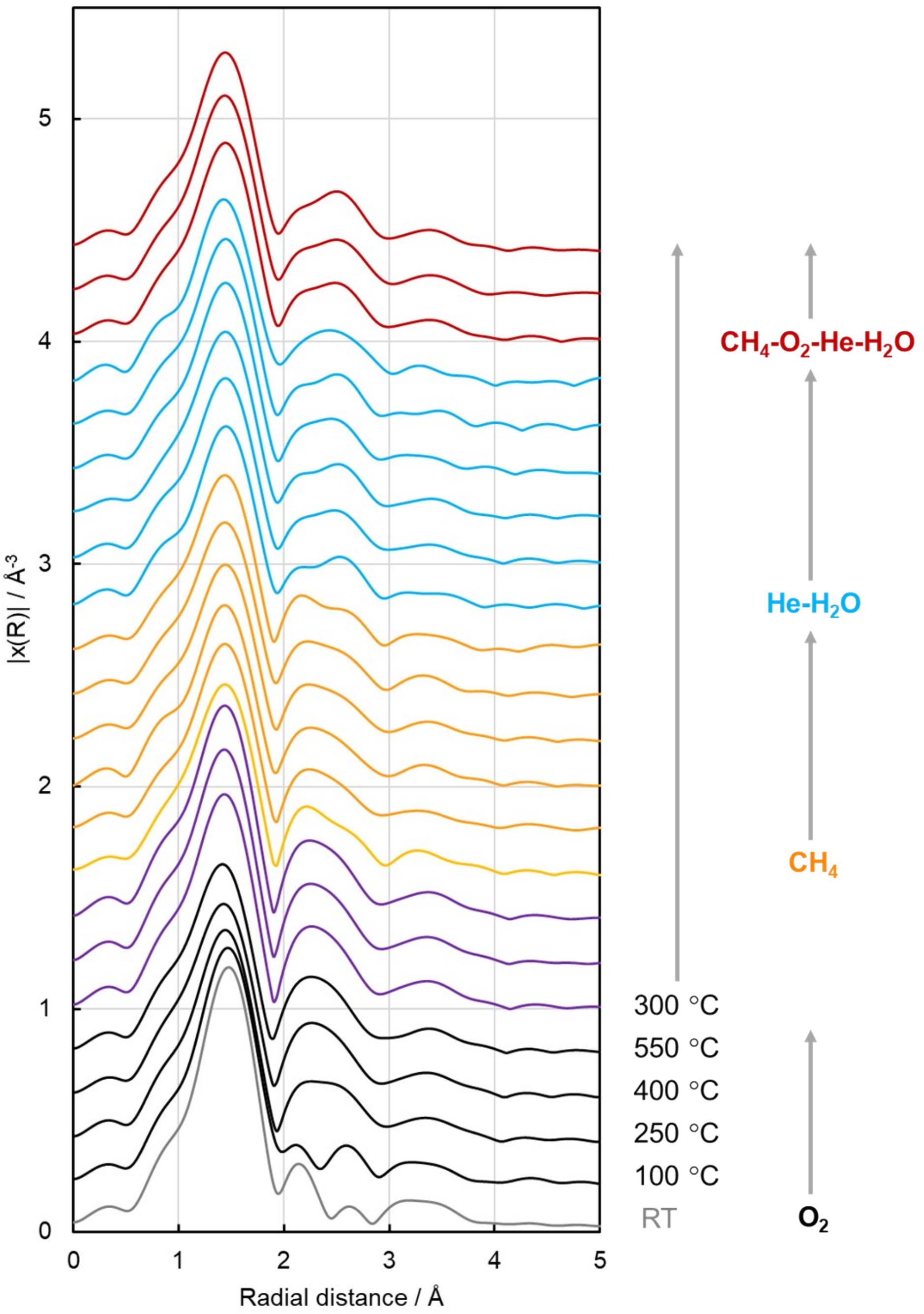

Figure S8 In-situ Cu K-edge FT EXAFS spectra of Cu2.0-MOR10 obtained according to Scheme S2. FT range: *k* = 3-10 Å.

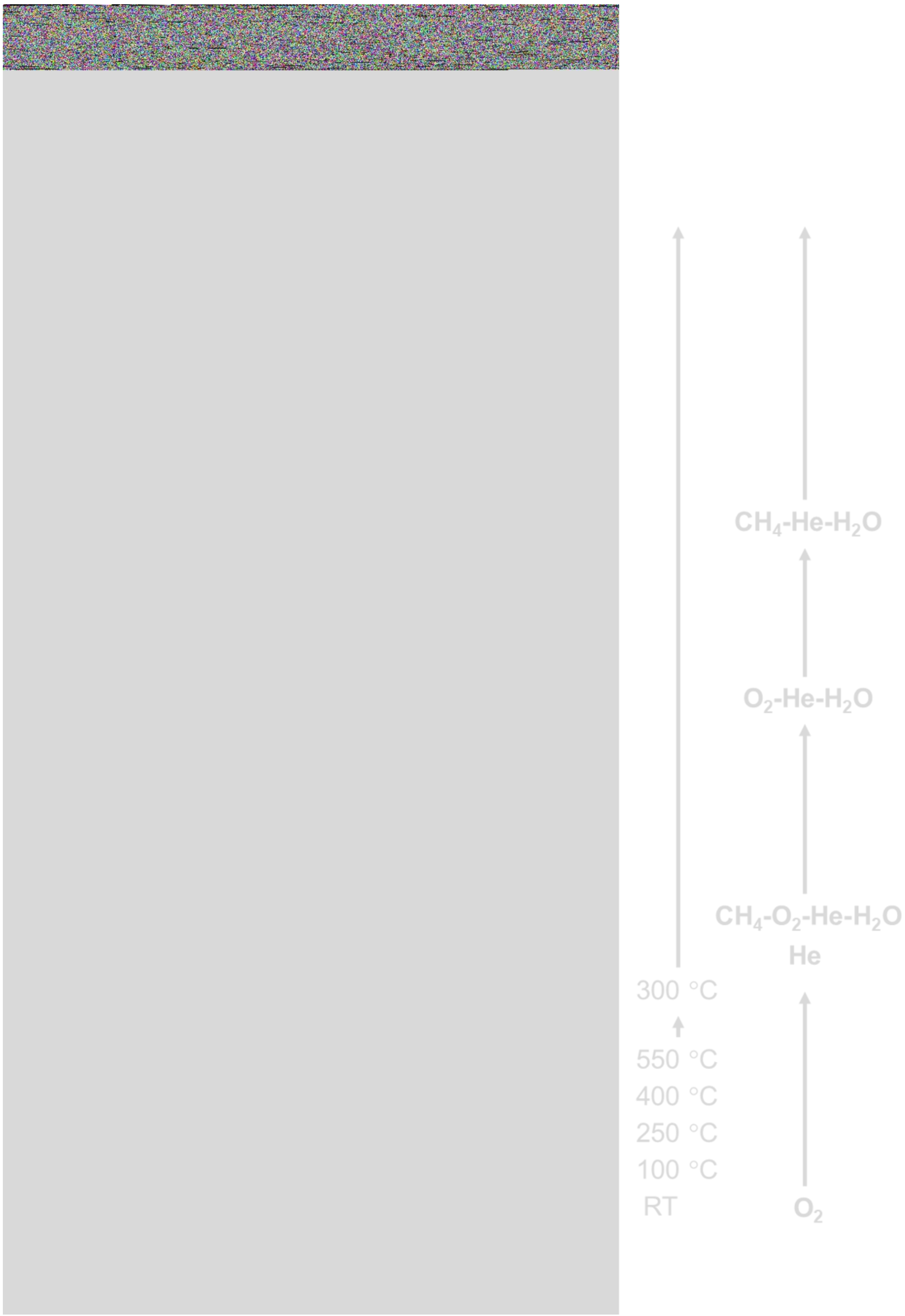

Figure S9 In-situ Cu K-edge FT EXAFS spectra of Cu1.1-FAU8 obtained according to Scheme S1. The EXAFS oscillations are shown in Figure S16(b). FT range: *k* = 3-9.3 Å.

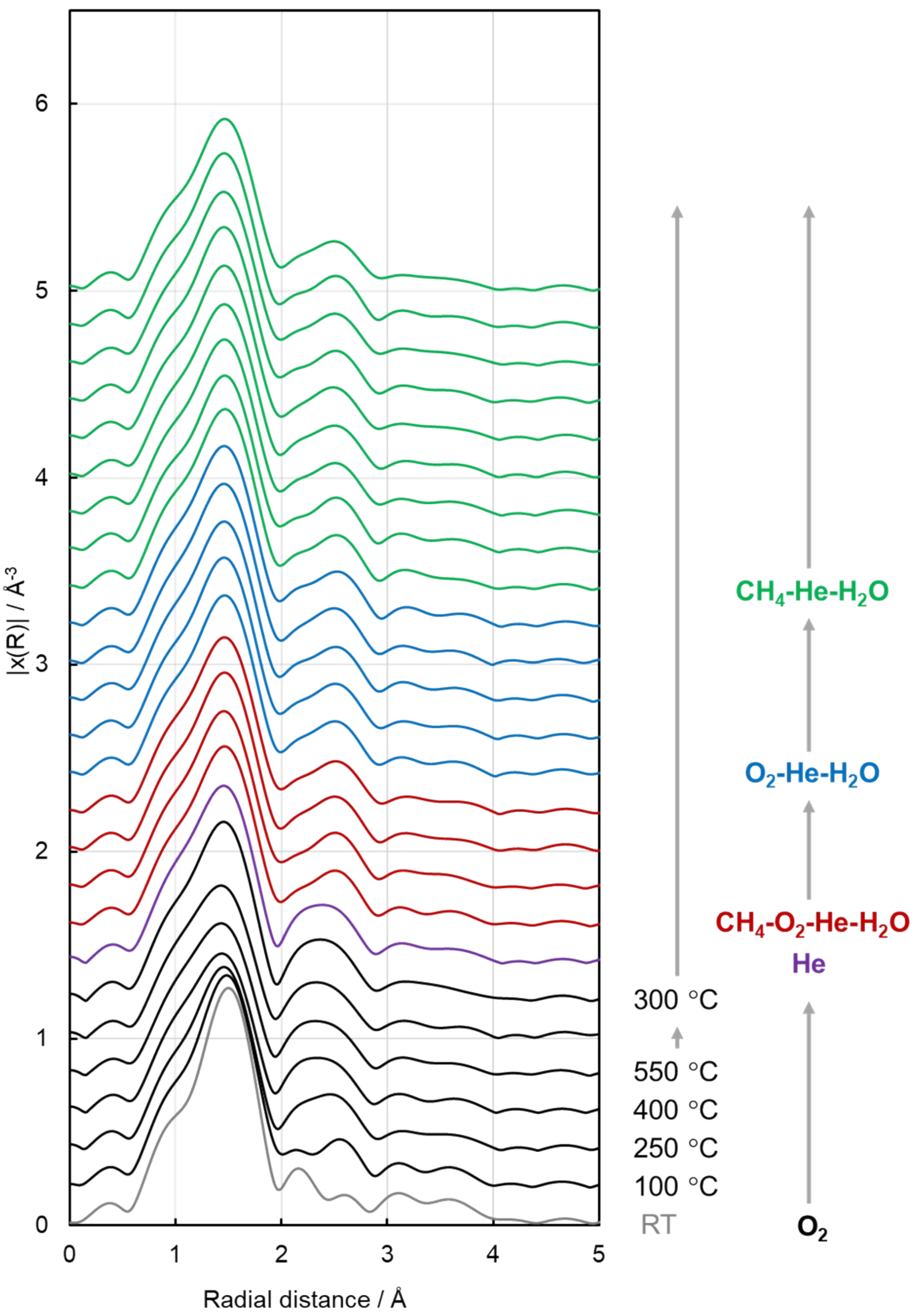

Figure S10 In-situ Cu K-edge FT EXAFS spectra of Cu2.3-MOR15 obtained according to Scheme S1. The EXAFS oscillations are shown in Figure S16(c). FT range: *k* = 3-10 Å.

Scheme S2 Experimental procedure for different control in-situ XAFS spectral measurements.

O_2 50 mL min^{-1} at 550 ºC (pretreatment)
↓
Cool to 300 ºC
↓
He 50 mL min^{-1}
↓
He 50 mL min^{-1}, H_2O(g)

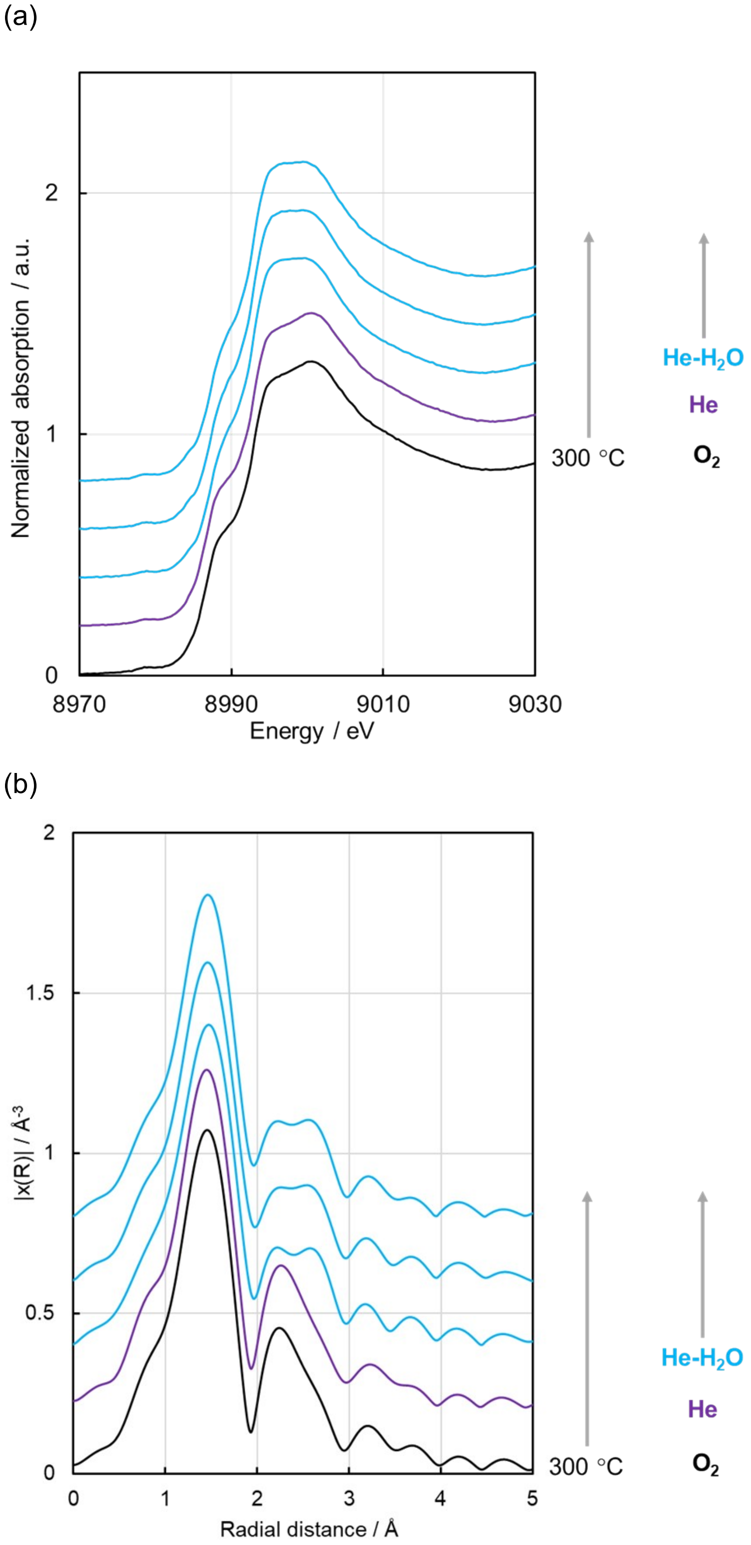

Figure S11 In-situ Cu K-edge (a) XANES and (b) FT EXAFS spectra of Cu2.0-MOR10 obtained according to Scheme S3. FT range: k = 3-10 Å.

Table S1. Structural parameters of Cu zeolite catalysts evaluated by the curve fitting analysis of *in situ* EXAFS spectra.[a]

Catalyst	Conditions	*CN*[b] (Cu-O)	*R*[c] (Cu-O)	*CN*[b] (Cu-Al)	*R*[c] (Cu-Al)	*CN*[b] (Cu-Cu)	*R*[c] (Cu-Cu)	E_0	σ^2[d]	R factor
Cu2.0-MOR10	Pretreated	3.6(9)	1.93(2)	1.1(6)	2.66(6)	0.2(7)	2.93(21)	8990.2(6)	0.0080(35)	0.0059
	(1)	3.8(2)	1.94(2)	0.7(4)	2.67(6)	0.6(5)	2.97(6)	8989.8(4)	0.0091(25)	0.0027
	(2)	3.7(5)	1.95(1)	0.8(3)	2.68(5)	0.5(4)	2.99(6)	8989.9(3)	0.0086(21)	0.0021
	(3)	3.7(6)	1.94(1)	0.7(3)	2.68(6)	0.5(4)	2.98(6)	8989.8(3)	0.0092(22)	0.0021
Cu1.1-FAU8	Pretreated	2.3(8)	1.92(2)	0.1(3)	2.55(36)	0.7(4)	2.91(5)	8988.2(35)	0.0044(43)	0.0111
	(1)	2.4(7)	1.92(2)	0.2(3)	2.54(12)	0.5(4)	2.93(5)	8988.1(29)	0.0045(36)	0.0084
	(2)	2.6(6)	1.92(2)	0.1(2)	2.47(15)	0.7(3)	2.90(3)	8987.9(23)	0.0061(31)	0.0041
	(3)	2.2(4)	1.92(1)	0.3(2)	2.51(6)	0.6(2)	2.92(3)	8988.4(20)	0.0043(26)	0.0043
Cu2.3-MOR15	Pretreated	3.4(11)	1.92(3)	0.7(8)	2.68(9)	0.3(9)	2.89(15)	8990.0(8)	0.0089(43)	0.0073
	(1)	3.6(8)	1.93(2)	0.5(6)	2.71(10)	0.5(7)	2.94(8)	8989.8(6)	0.0097(32)	0.0039
	(2)	3.7(8)	1.93(2)	0.5(6)	2.69(10)	0.6(7)	2.94(7)	8989.8(6)	0.0095(32)	0.0040
	(3)	3.4(7)	1.94(2)	0.6(5)	2.72(8)	0.3(6)	2.94(10)	8989.9(5)	0.0092(29)	0.0034
Cu2.0-MOR10	Wet He	3.6(3)	1.95(1)	0.8(2)	2.69(3)	0.5(3)	2.99(3)	8989.9(2)	0.0091(13)	0.0007

[a] FT range: 3-10 Å^{-1} for Cu2.0-MOR10 and Cu2.3-MOR15; 3-9.3 Å^{-1} for Cu1.1-FAU8. Curve fitting range: 1.0-3.0 Å. The number of independent points ($N_{ind} = 2(k_{max} - k_{min})(R_{max} - R_{min})/\pi$) is larger than the number of structural parameters used for the analysis in this study where identical E_0 and σ^2 are assumed for the three scatterings of Cu-O, Cu-Al, and Cu-Cu. [b] Coordination number. [c] Atomic distance. [d] Debye-Waller factor.

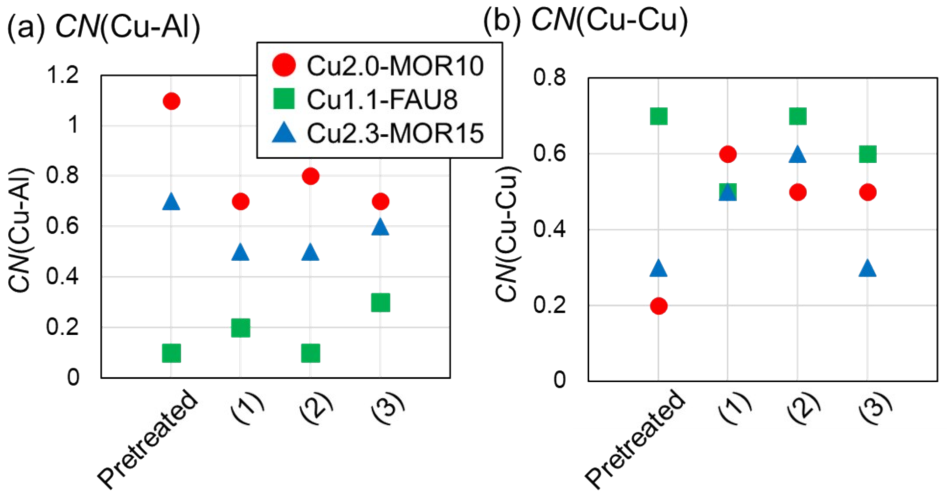

Figure S12. Variation of CN(Cu-Al) and CN(Cu-Cu) of Cu2.0-MOR10 (red circle), Cu1.1-FAU8 (green square), and Cu2.3-MOR15 (blue triangle) with the gas flow conditions.

(a) Cu2.0-MOR10

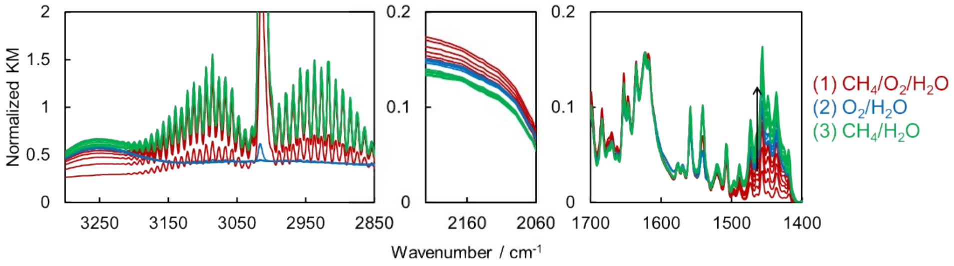

(b) Cu1.1-FAU8

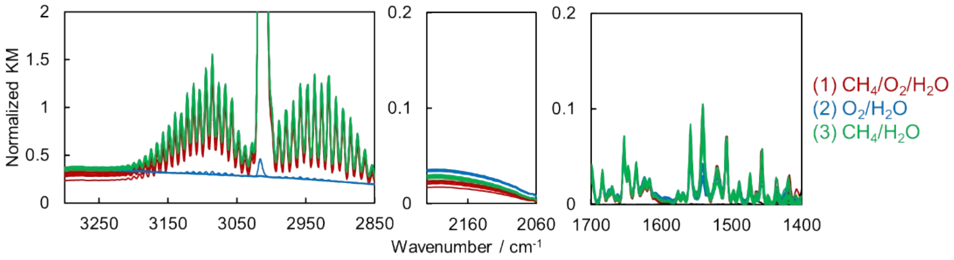

(c) Cu2.3-MOR15

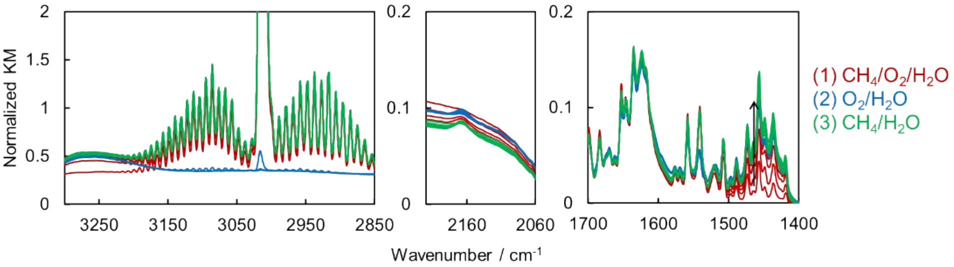

(d) Cu2.0-MOR10 under CH_4/O_2

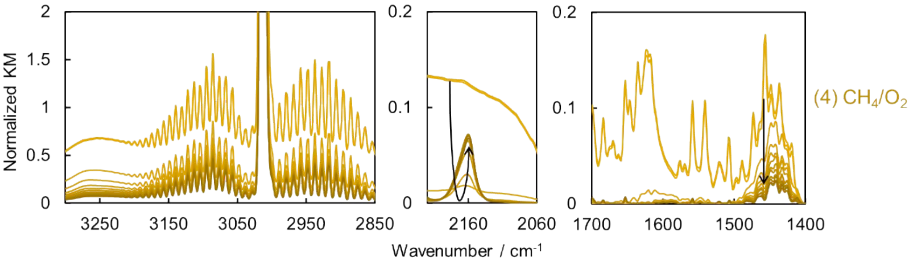

Figure S13. Absorption-normalized in-situ DRIFT spectra obtained for (a) Cu2.0-MOR10, (b) Cu2.3-MOR15 and (c) Cu1.1-FAU8 under gas flow conditions (1) (red line), (2) (blue line) and (3) (green line). (d) DRIFT spectra of Cu2.0-MOR10 measured under (4) CH_4/O_2 after (3). Spectra in (a)–(d) were normalised by the intensity of the band related to the vibration/rotation of CH_4, which was determined by subtracting the intensity at 2937 cm^{-1} at the end of gas flow conditions (2) from that of (1).

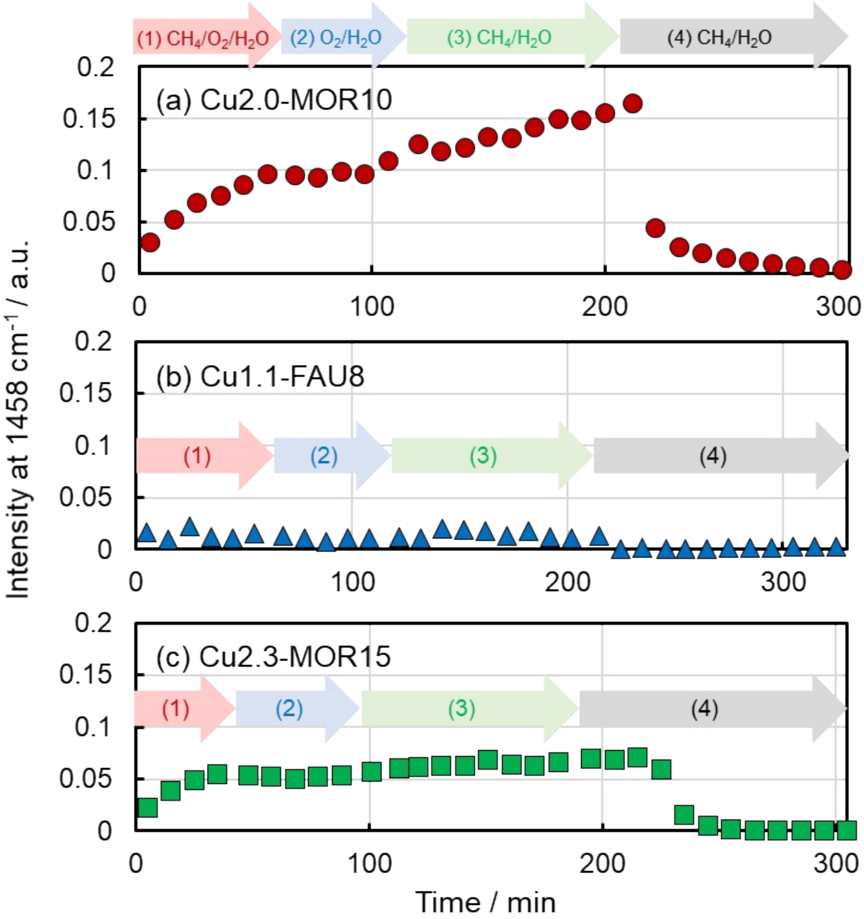

Figure S14. Variation of normalize IR adsorption intensity at 1458 cm^{-1} of (a) Cu2.0-MOR10 (red circles), (b) Cu1.1-FAU8 (blue triangles) and (c) Cu2.3-MOR15 (green squares) under the flow conditions (1) to (4).

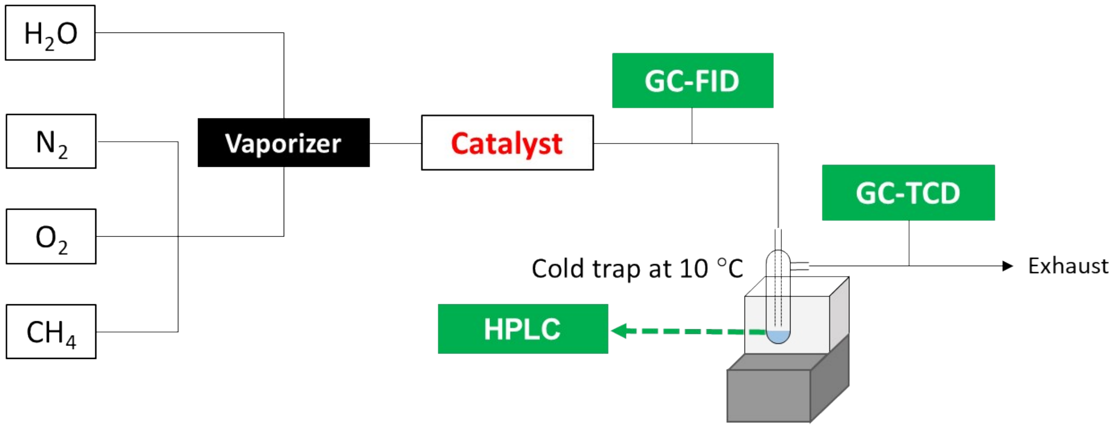

Figure S15. Schematic diagram of catalytic reaction and product analysis system used in this study.

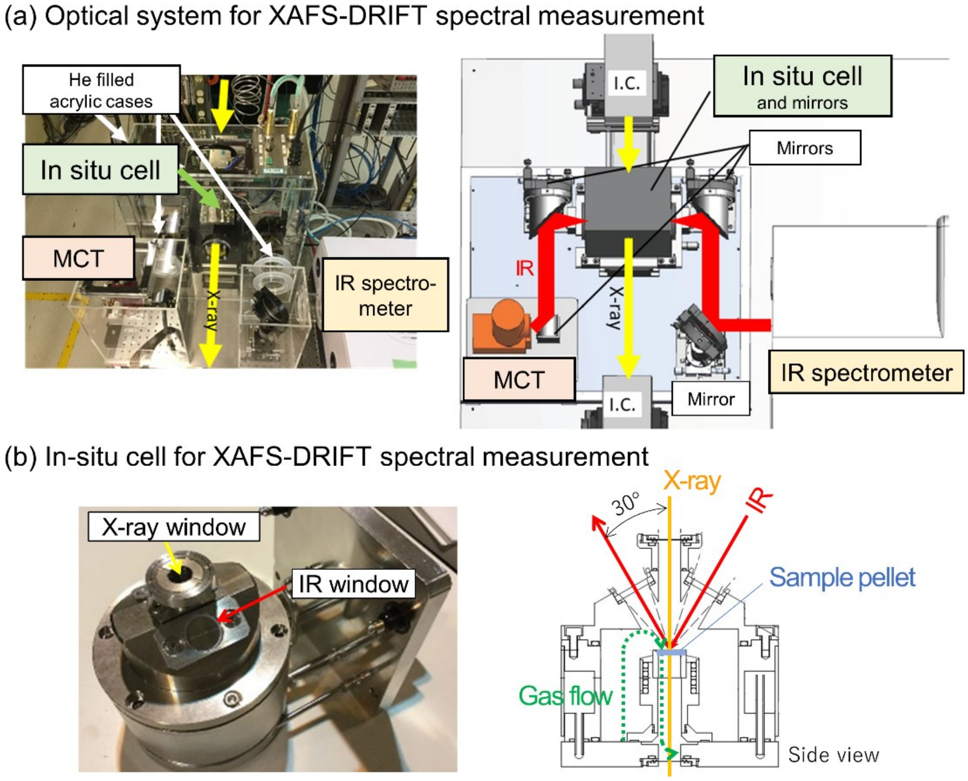

Figure S16. Photographs and schematics of the (a) optical system and (b) in-situ cell for the in-situ XAFS and DRIFT spectral measurements at BL01B1 of SPring-8.

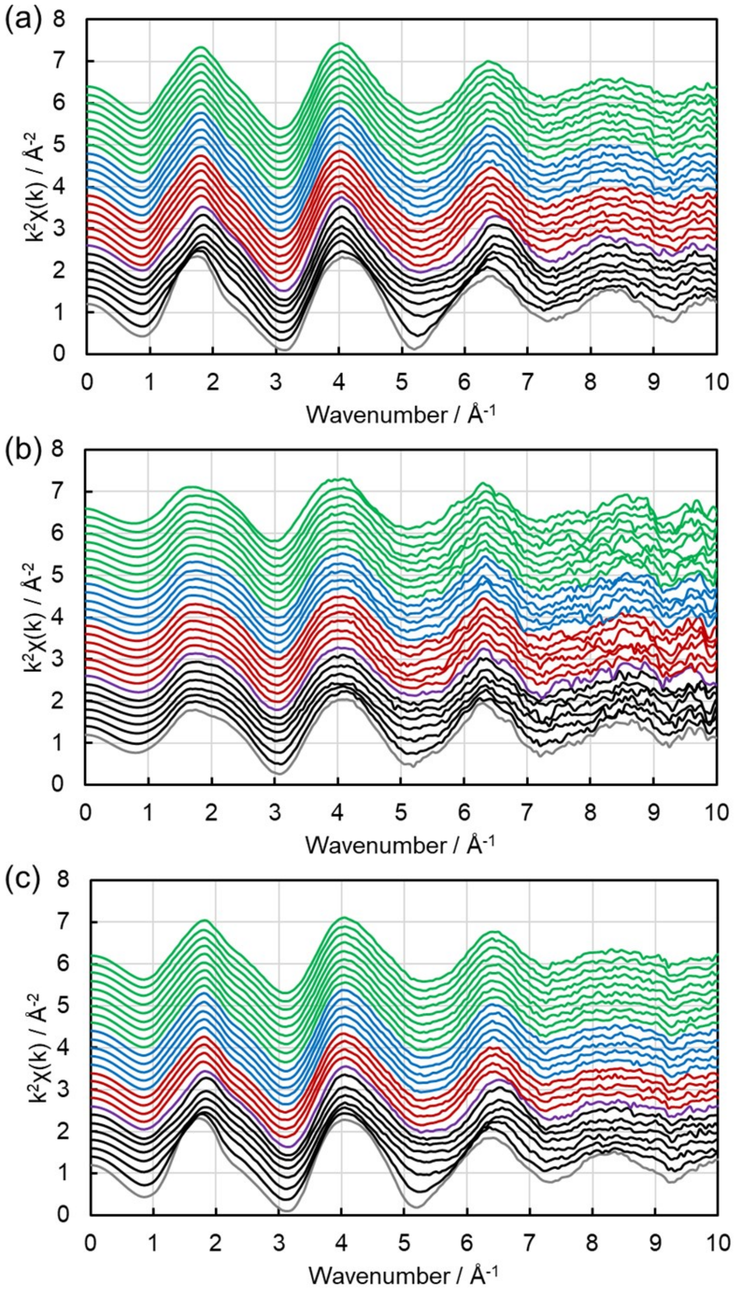

Figure S17. EXAFS oscillations corresponding to Figure S7, S9, and S10.